Applied Geochemistry 41 (2014) 163–175

Contents lists available at ScienceDirect

Applied Geochemistry

journal homepage: www.elsevier.com/locate/apgeochem

Source of groundwater salinity in coastline aquifers based on environmental isotopes (Portugal): Natural *vs.* human interference. A review and reinterpretation

Paula M. Carreira [a,*], José M. Marques [b], Dina Nunes [a]

[a] Campus Tecnológico e Nuclear, Instituto Superior Técnico, Universidade Técnica de Lisboa, Estrada Nacional 10, ao km 139,7, 2695-066 Bobadela LRS, Portugal
[b] CEPGIST/CERENA, Instituto Superior Técnico, Universidade Técnica de Lisboa, Av. Rovisco Pais, 1049-001 Lisboa, Portugal

ARTICLE INFO

Article history:
Received 7 June 2013
Accepted 16 December 2013
Available online 19 December 2013
Editorial handling by M. Kersten

ABSTRACT

Environmental stable ($\delta^{18}O$, $\delta^{2}H$, $\delta^{13}C$) and radioactive (^{3}H and ^{14}C) isotopes, together with geochemical data were used to identify the origin of salinization in different environments. Three case studies from sedimentary basins of continental Portugal are presented: (i) two at the Meso-Cenozoic Portuguese southern border (Algarve basin) and (ii) one at the Lower Tagus–Lower Sado basin (central Portugal), with a new data interpretation. Groundwater salinization occurs in all three cases, and may reach values of several grams of Total Dissolved Solids per liter; above accepted limits for drinking water. The source of this high mineralization could be: (a) seawater intrusion (ancient or modern); (b) dissolution from diapiric structures intruding on the aquifer systems; (c) brine dissolution at depth; and (d) evaporation of irrigation water. The results obtained have provided an effective label for seawater and freshwater, to enable seawater intrusion to be traced, as well as the identification of other processes that might be responsible for groundwater salinization, such as salt minerals dissolution and ion exchange.

1. Introduction

Steady increase in the salinity of most of the major aquifers being used for water supply in coastal regions, in particular in areas under arid and semi-arid conditions, provide evidences of water quality deterioration (e.g., Shi et al., 2001; Kim et al., 2003; Cartwright et al., 2004; Pulido-Leboeuf, 2004; Klein-BenDavid et al., 2005; Jalali, 2007; Bouchaou et al., 2008). This increase in mineralization of groundwater resources is often due to inflow of saline (dense) water, during heavy withdrawals of fresh water from coastal aquifers, and/or mobilization of saline formation waters by overexploitation of inland aquifer systems. Not only seawater mixing is responsible for water resource degradation. Water pollution due to extensive irrigation and the use of fertilizers and other pesticides is also growing all over the world. As a consequence of the different income sources for groundwater quality deterioration, it is necessary to identify and characterize the specific processes involved. Among the different approaches, isotope techniques are particularly effective for identifying the source of salinity and renewability of groundwater all over the world (e.g., Carreira, 1991; Cabral et al., 1992; Carreira et al., 1994, 2010; Gaye, 2001; Kim et al., 2003; Cartwright et al., 2006; Möller et al., 2007; Bouchaou et al., 2008; Carol et al., 2009; Koh et al., 2012).

The differences observed between the stable isotopic composition of groundwater and that of local precipitation composition can be due to: (i) different recharge episodes; (ii) to different recharge sources (for example surface waters and precipitation) or (iii) even to contamination inputs by mixing processes between different aquifer systems, which can lead to an isotopic deviation between groundwater and local precipitation.

On the Portuguese mainland, seawater intrusion has been described along the Atlantic coast from Aveiro, in the N of Portugal, to Algarve in the S, usually in relation with sedimentary basins. In these areas, the overexploitation of groundwater has resulted in salinization extending inland. This has worsened in recent decades, especially during the summer months when both the local population is boosted by significant numbers of tourists and demand for irrigation water peaks.

In this paper three case studies will be presented, where the main goals were to identify and understand the importance that different salt origins (ancient or modern seawater intrusion, dissolution of evaporitic minerals) could have on the groundwater quality deterioration for human uses and the characterization of the specific processes involved.

Environmental isotope studies were applied in order to assess the origin of salinization. These were complemented by geochemical investigations, which in some cases were not able to resolve the questions. Both regions (Algarve and Sado groundwater systems) are found near the coastline, within sedimentary basins where the presence of evaporitic minerals dispersed or

* Corresponding author. Tel.: + 351 219946179; fax: + 351 219946185.
E-mail addresses: carreira@ctn.ist.utl.pt (P.M. Carreira), jose.marques@ist.utl.pt (J.M. Marques).

0883-2927/$ - see front matter © 2013 Elsevier Ltd. All rights reserved.
http://dx.doi.org/10.1016/j.apgeochem.2013.12.012

concentrated in the geological layers is not unusual. Three case studies on coastal aquifers will be presented: (i) two at the Meso-Cenozoic Portuguese S border (Algarve basin), and (ii) a third one at the Lower Tagus–Sado sedimentary basin (central Portugal). In all these case studies groundwater salinization occurs, reaching values of several grams of Total Dissolved Solids (TDS)/L. Based on the geological features of each area the source of this high mineralization could be ascribed to: (a) seawater intrusion; (b) dissolution of diapiric structures, intruding the aquifers, or spreading saline minerals; (c) brine dissolution at depth or mixing with ancient seawater and (d) evaporation of irrigation water.

2. Analytical methodology

2.1. Background

A qualitative and quantitative characterization of groundwater recharge is essential to ensure the sustainable development and management of groundwater resources. A reliable estimate of recharge rate can be obtained on the basis of classical approaches, such as water level monitoring (Custódio and Llamas, 1983). However, examination of isotopic composition allows a differentiation of recharge and even precipitation sources, and hence of recharge mechanisms (Fig. 1a). Isotopic composition of groundwater ($\delta^{18}O$ and $\delta^{2}H$ values) is defined by the isotopic signatures of recharge. If most of the recharge is derived from direct infiltration of precipitation, the groundwater will reflect the isotopic composition of that precipitation (Craig, 1961; Dansgaard, 1964; Rozanski et al., 1992; Gourcy et al., 2005). However, if most of the recharge is derived from surface water (rivers or lakes) instead of precipitation, the groundwater will reflect the mean isotopic composition of the contributing river or lake waters. On the other hand, it should be noted that in some cases the isotopic composition of precipitation may be close to that of river waters (Fritz, 1981). However in large and sometimes in small basins rainfall isotopic composition

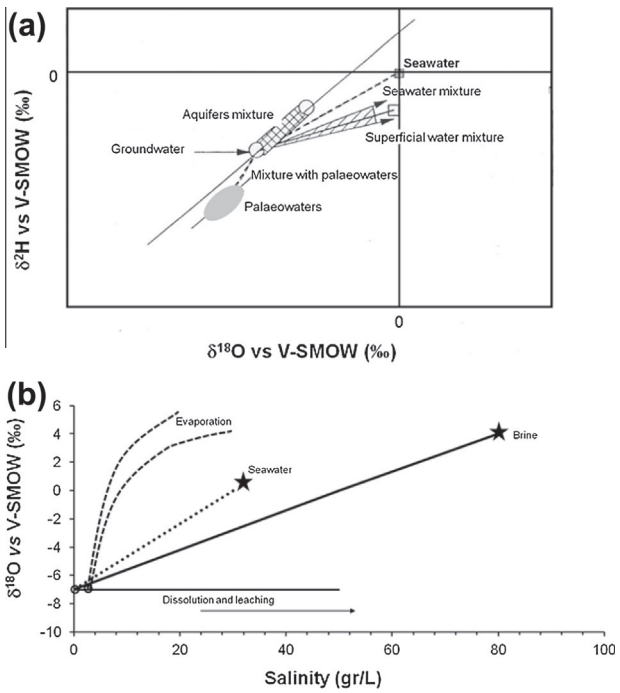

Fig. 1. (a) $\delta^{2}H$ *vs.* $\delta^{18}O$: change in isotopic composition of the groundwater associated with different processes (adapted from Gat, 1981). (b) $\delta^{18}O$ *vs.* salinity: change in isotopic composition of water, ascribed to different salinization processes (adapted from Gonfiantini and Araguás, 1988).

can diverge, and the river will be a proportional mixing of all rainfall contributions (Mas-Pla et al., 2013). This deviation (surface waters–groundwaters) will be more perceptible when a topographic gradient is well defined.

Stable isotopes provide an effective label for seawater and freshwater, to enable tracing of seawater intrusion, as well as identifying other processes that might be responsible for groundwater salinization. Evolution of stable isotope concentration of water during different processes related to water salinization is presented in Fig. 1b. In studies dealing with seawater intrusion and the identification of groundwater salinization processes, it is common to consider both isotopic and hydrochemical evolution. Such an approach enables the salinization process (or processes) to be clearly distinguished, for cases where freshwater salinity may be caused by direct seawater intrusion, leaching of salt formations, mineral dissolution, or salt accumulation due to evaporation (Aráguás-Aráguas and Gonfiantini, 1989; Edmunds and Droubi, 1998; Yurtsever, 1997). During salt formation or mineral dissolution processes, the stable isotope content of the water is not affected but water salinity increases (Fig. 1b). This is a unique feature that enables identification of such processes based on isotopic and geochemical data.

In hydrological settings in which groundwater is old (>10,000 years), regional climatic conditions at the time of recharge may have been different from those existing today, and this is reflected in the isotope composition of the groundwater. The present-day characteristic values in ^{18}O and in ^{2}H observed in precipitation may be used as sensitive indicators of change and complexity in past temperatures, precipitation patterns and air masses circulation. Past rainfall stored as palaeogroundwater, provide evidences of former climatic conditions. Climatic changes are expressed primarily as (i) isotopic depletion relative to modern groundwaters with reference to the meteoric water line; (ii) change in deuterium excess, signifying changes in humidity in the air mass as it detaches from its primary oceanic source moving over arid regions; and (iii) local condensation and evaporation effects within the colds or in falling rain (Rozanski et al., 1992; Edmunds, 2005).

Moreover, if the flow regime is simple and mixing is negligible, the aquifers can serve as archives of information about environmental conditions at the time of recharge (e.g., Rozanski, 1985; Rozanski et al., 1992; Darling et al., 1997; Edmunds and Droubi, 1998; Edmunds, 2005; Bouchaou et al., 2008). The stable isotopes of hydrogen and oxygen in palaeowaters (groundwater recharged under climate conditions different than today) reflect the air temperature at land surface and the air mass circulation (origin of moisture) at the time of precipitation and infiltration (e.g., Rozanski, 1985; Stute et al., 1995; Edmunds, 2005). Therefore, dating groundwater will help in the identification of the seawater intrusion mechanism, i.e., if we are dealing with modern or ancient salt water bodies such as seawater, brackish or brine waters.

Groundwater dating with ^{14}C is not an easy procedure, in particular in carbonate aquifers or even when carbonate layers are present within the geological strata, as occurs in the Lower Sado–Lower Tagus sedimentary basin. In a simple approach to carbon-14 dating of groundwater systems it is assumed that ^{14}C "travels" with the water molecules along the flow path, and that the main mechanism that is changing the ^{14}C content of the groundwater (Total Dissolved Inorganic Carbon – TDIC) is "pure" radioactive decay. However, the isotopic signature of the ^{14}C may be diluted, particularly by ^{14}C-free sources, leading to apparent groundwater ages higher than reality (Carreira et al., 2008).

A common and straightforward way to estimate the initial ^{14}C activity is by relating the $\delta^{13}C$ content of the DIC in the groundwater to the mixed carbon from carbonate rocks, using carbon from soil CO_2 and a fractionation factor between the different carbonate

phases as a function of temperature (Salem et al., 1980; Gonfiantini and Zuppi, 2003). The equation proposed by these authors is the following and was used to estimate the apparent radiocarbon ages of the groundwater samples from Lower Tagus–Lower Sado basin:

$$t = 8267 \ln(C_o/C) \quad (1)$$

and

$$C_o = [100(\delta_{TDIC} - \delta_R)(1 + 2.3\varepsilon_{13}/1000)]/(\delta_S - \delta_R + \varepsilon_{13}) \quad (2)$$

The apparent carbon-14 groundwater age was estimated using the $\delta^{13}C$ value as a correction factor, assuming a closed model where t is time (age), C is the measured ^{14}C activity and C_o is the "initial" ^{14}C activity in the (TDIC) in the measured groundwater (expressed in pmC). It has been assumed that the ^{14}C activity of the soil CO_2 is equal to 100 pmC. δ_{TDIC} is the measured ^{13}C content of soil CO_2, δ_R is the ^{13}C content of $CaCO_3$ in the soil and in the rock matrix, δ_S represents the ^{13}C content of soil CO_2 whereas ε_{13} stands for the ^{13}C enrichment factor during dissolution of soil CO_2 in the infiltrating water.

2.2. Sampling and analytical methods

Concerning the three case studies described in Section 1: a total of 74 water samples were collected in Algarve basin (Fig. 2; Table 1). Within the Portimão–Estombar area two sampling campaigns were performed. The O and H stable isotope composition of the water samples were determined using a Finnigan Mat 250 and VG Micromass, following the analytical methods of Friedman (1953) and Epstein and Mayeda (1953), with an accuracy of ±1‰ for δ^2H and ±0.1‰ for $\delta^{18}O$.

The tritium (^3H) content was determined using the electrolytic enrichment and liquid scintillation counting method (IAEA, 1976; Lucas and Unterweger, 2000) using a Packard Tri-Carb 2000 CA/LL. The error associated with the ^3H measurements (usually around 0.6 tritium units (TU)) varies with the ^3H concentration in the sample.

At the Lower Tagus–Lower Sado basin a total of 40 boreholes waters were sampled in different field work campaigns. Stable isotopes (^2H, ^{13}C and ^{18}O) were measured using a SIRA 10 mass spectrometer from VG ISOGAS following the analytical methods of Friedman (1953) and Epstein and Mayeda (1953), while ^{13}C and ^{14}C determinations were made on the TDIC (Total Dissolved Inorganic Carbon) of groundwater, precipitated in the field as $BaCO_3$ at a pH higher than 9.0. The counting rates of the ^{14}C (benzene) were measured using a liquid scintillation counter (PACKARD TRI-CARB 4530). ^{14}C content is expressed in pmC (percentage of modern carbon). The errors associated with this method vary with the amount of carbon available in each sample, and increase where ^{14}C content is low. The ^{13}C values are reported in ‰ to V-PDB (Vienna–Peedee Belemnite) standard, with an accuracy of ±0.1‰.

In all water samples, major elements were determined in the National Water Authority laboratories, using the following methods: atomic absorption for Ca^{2+} and Mg^{2+}; emission spectrometry for Na^+, K^+, and ion chromatography for SO_4^{2-}, NO_3^- and Cl^-.

The program HIDSPEC, a hydrogeochemical model that calculates the speciation of natural waters (Carvalho and Almeida, 1989), was used to calculate the saturation indexes (SI) of the waters with respect to calcite, dolomite and gypsum. The same program was applied to calculate the ionic balance for each water sample; the errors range from 0.3% up to 6.7%.

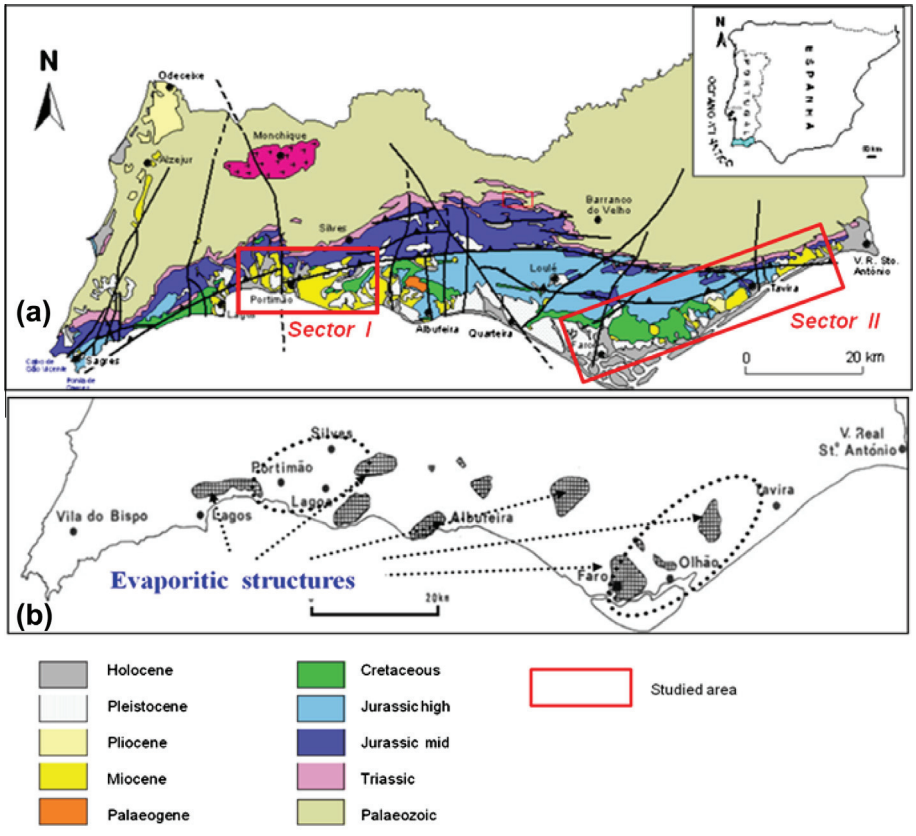

Fig. 2. (a) Geological map of Algarve basin showing the two selected sectors (adapted from Lopes, 2006). (b) Location of the most important diapiric structures in Algarve basin (adapted from Costa et al., 1985).

Table 1
Algarve basin, south of Portugal: physico-chemical and isotopic data ascribed to the groundwater sampling sites in Portimão–Estombar and Faro–Tavira area.

Portimão–Estombar						Faro–Tavira											
Sample	EC (μS/cm)	Cl (mg/L)	$\delta^{18}O$ (‰)	$\delta^{2}H$ (‰)	$^{3}H \pm \sigma$ (TU)	Sample	EC (μS/cm)	Cl (mg/L)	$\delta^{18}O$ (‰)	$\delta^{2}H$ (‰)	$^{3}H \pm \sigma$ (TU)	Sample	EC (μS/cm)	Cl (mg/L)	$\delta^{18}O$ (‰)	$\delta^{2}H$ (‰)	$^{3}H \pm \sigma$ (TU)
61(*)	4160	1150.2	−3.99	−24.7	4.8 ± 0.2	1(*)	940	119.5	−4.35	−24.2	8.7 ± 0.4	26(*)	1400	236.6	−4.28	−24.8	3.3 ± 0.4
62(*)	2920	788.1	−3.79	−24.0		2(*)	1300	203.8	−4.52	−24.9	1.3 ± 0.3	27(*)	700	106.5	−4.57	−26.3	14.5 ± 0.5
63(*)	1490	305.3	−4.29	−24.1	4.0 ± 0.2	3(*)	960	119.5	−4.50	−25.7		28(*)	740	120.7	−4.12	−22.6	
64(*)	840	92.3	−4.26	−27.3		4(*)	1200	147.6	−4.42	−24.6		29(*)	700	49.7	−4.30	−24.1	
65(*)	792	85.2	−4.38	−26.2	7.8 ± 0.3	5(*)	2680	688.8	−4.35	−23.8		30(*)	750	56.8	−4.40	−26.7	12.5 ± 0.4
67(*)	660	63.9	−4.14	−26.2	10.9 ± 0.3	6(*)	1500	232.0	−4.37	−25.3	1.3 ± 0.3	31(*)	670	56.8	−4.37	−25.2	
71(ϕ)	850	106.5	−4.27	−24.8	5.4 ± 0.3	7(*)	750	53.0	−4.26	−22.7		32(*)	1200	49.7	−4.41	−25.1	
72(ϕ)	7700	2414.0	−3.58	−22.3	6.5 ± 0.4	8(*)	3300	866.2	−4.21	−23.2	2.2 ± 0.3	33(*)	890	99.4	−4.33	−24.9	10.6 ± 0.3
73(ϕ)	6250	1874.4	−3.78	−22.9	5.7 ± 0.4	9(*)	1000	120.7	−4.63	−24.8		34(*)	800	78.0	−4.44	−25.8	
74(ϕ)	10,150	3280.2	−3.49	−21.5	4.8 ± 0.4	10(*)	1080	177.5	−4.32	−27.8		35(*)	3830	1032.6	−3.96	−23.1	
75(ϕ)	10,200	3294.4	−3.45	−20.9	5.5 ± 0.4	11(*)	910	142.0	−4.45	−27.2	7.7 ± 0.4	36(*)	640	35.5	−4.35	−26.9	
78(*)	892	127.8	−4.16	−25.7	5.8 ± 0.4	12(*)	1500	284.0	−4.45	−27.4	6.0 ± 0.4	37(*)	1500	372.9	−4.29	−22.8	
61a(*)	1406		−4.36			13(*)	1670	319.5	−4.35	−26.5		38(*)	1610	308.4	−3.34	−20.5	8.3 ± 0.3
62a(*)	5040		−3.94			14(*)	1060	142.0	−4.60	−27.6	5.6 ± 0.4	39(*)	6950	2294.7	−4.27	−24.9	0.6 ± 0.3
63a(*)	1768		−4.23			15(*)	1150	177.5	−4.60	−27.4		40(*)	920	120.7	−4.33	−28.4	
64a(*)	921		−3.71			16(*)	1030	127.0	−4.45	−27.4		41(*)	910	142.0	−4.78	−27.3	6.5 ± 0.2
71a(ϕ)	1067		−4.12			17(*)	1260	189.8	−3.97	−23.7	8.6 ± 0.4	42(*)	2100	494.7	−4.21	−25.6	9.7 ± 0.3
72a()	7250		−3.59			18(*)	3050	787.3	−4.22	−27.2		43(*)	5800	1721.0	−4.25	−24.7	4.2 ± 0.2
74a(ϕ)	10,130		−3.34			19(*)	2100	337.4	−4.50	−26.9		44(ϕ)	9550	2946.5	−3.74	−19.8	7.6 ± 0.4
78a(*)	1056		−4.18			20(*)	1350	246.0	−4.39	−25.4	5.6 ± 0.4	45(*)	5500	1548.9	−4.00	−23.7	7.6 ± 0.3
99(*)	6300		−3.84			21(*)	1100	140.6	−4.37	−27.4	2.4 ± 0.4	46(*)	3800	867.6	−4.24	−25.6	
101(*)	980		−4.22			22(*)	1300	239.0	−4.32	−25.2		47(*)	1540	243.8	−4.19	−24.8	6.6 ± 0.3
102(*)	998		−4.16			23(*)	1040	161.7	−4.21	−24.8	8.9 ± 0.4	48(*)	3800	989.6	−4.45	−25.0	4.5 ± 0.3
72b(ϕ)	7240		−3.63			24(*)	1200	217.9	−4.09	−25.6		49(*)	2280	516.3	−4.53	−27.4	
						25(*)	800	84.4	−4.32	−25.8		50(*)	1300	308.3	−4.59	−25.3	3.9 ± 0.3

Notes: (ϕ) stands for spring and (*) for borehole waters.

3. Case study: Algarve sedimentary basin–southern Portugal (Portimão–Estombar and Faro–Tavira)

3.1. Hydrogeological setup

The Algarve basin is located in the south of the Portuguese mainland and is characterized by a warm Mediterranean climate. From the hydrogeological point of view this sedimentary basin is mainly composed of Tertiary karstified limestones and Quaternary alluvial deposits, which represent the main water bearing formations in the Algarve coastal belt. Along the southern coast, intensive exploitation of existing karst aquifers, plus the occurrence of diapiric tectonics and disseminated salt diapir intrusions, may bring about problems of exhaustion and quality degradation of local/regional groundwater systems. Although aquifer potential is high, the large demands made by irrigated agriculture and tourism make fresh water a scarce commodity. In this region severe groundwater salinization occurs, and may reach values of several grams of TDS/L. There are two main sources of solutes: (i) seawater intrusion as a consequence of intense exploitation and, (ii) dissolution of several diapir structures (of evaporitic origin) intruded in the aquifers, or of dispersed evaporitic minerals such as halite and gypsum.

3.2. Results and discussion

More than 150 borehole and spring waters were regularly sampled around the Algarve coast, between Portimão on the West and the Spanish border on East (Fig. 2), though in the present study only results from 65 selected sampling points will be discussed. The field work was performed between 1986 and 1989. The electrical conductivity of the groundwater samples range from 500 up to 10,500 μS/cm. The $\delta^{18}O$ composition was determined in all water samples, while $\delta^{2}H$ and ^{3}H were only measured in the samples from the first field work campaign. Seawater was collected in order to calculate the mean isotopic composition of the Atlantic ocean around the south of Portugal the values obtained are: $\delta^{2}H = 4.5 \pm 2.7$‰ ($n = 10$) and $\delta^{18}O = 0.98 \pm 0.3$‰ ($n = 28$). The mean electrical conductivity was 51,704 ± 2400 μS/cm ($n = 28$).

In a considerable number of sampling sites the groundwater salinity and isotopic content vary significantly with time, although not always with similar trends. The initial research area was subdivided in four zones based on the structural geology and main groundwater flow directions (Costa et al., 1985; Silva et al., 1986). In this paper the results presented and discussed are ascribed only to two areas: Portimão–Estombar and Faro–Tavira (Fig. 2), since these sectors present the greater groundwater salinization problems where the isotopic data interpretation was crucial in the identification of the origin of salinization processes (Table 1).

(i) *Case Study I: Portimão–Estombar*

In the first sector situated near Portimão, in the W part of the Algarve basin, several karst springs can be found issuing along Arade river banks, near Estombar. Groundwater samples were collected from Estombar springs as well as from boreholes that were drilled through the karstic aquifer in the same locality. In all groundwater samples, isotopic composition ($\delta^{2}H$ and $\delta^{18}O$) was determined and field parameters such as electrical conductivity, pH and temperature were measured *in situ*.

Plotting the isotopic data ($\delta^{2}H$ *vs.* $\delta^{18}O$) (Fig. 3a) or the $\delta^{18}O$ values as a function of electrical conductivity (Fig. 3b), the groundwater samples (Estombar springs and part of the boreholes) are displayed along a seawater–fresh water mixing line, as clearly shown by the correlation between oxygen-18 and electrical conductivity (Fig. 3b). In both diagrams, the theoretical seawater–fresh water mixing line and the regression line drawn through the data points almost overlap, indicating clearly that the groundwater samples are the result of a mixture of seawater and fresh water. Using the mean isotopic composition of the seawater samples ($\delta^{2}H = 4.5$‰ and $\delta^{18}O = 0.98$‰) collected along the Algarve

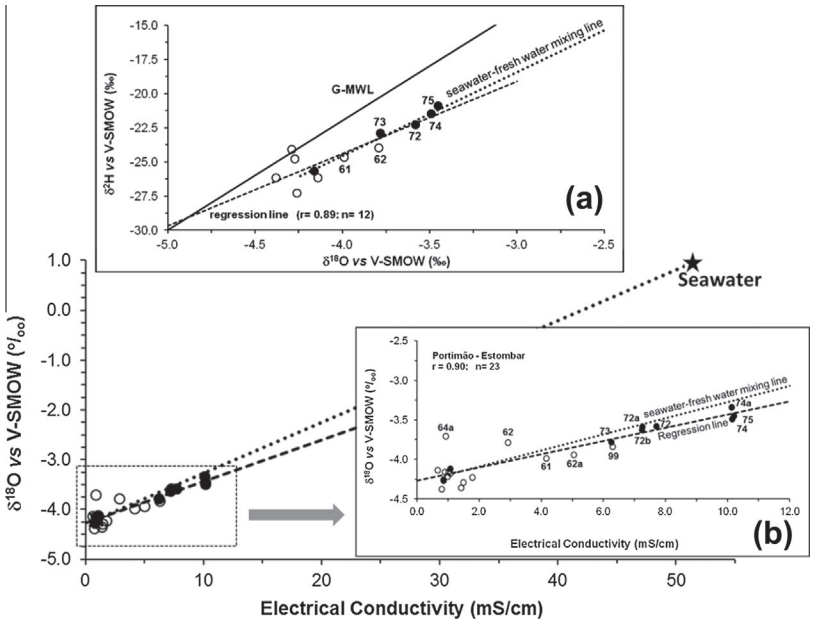

Fig. 3. (a) δ^2H *vs.* $\delta^{18}O$; (b) $\delta^{18}O$ *vs.* electrical conductivity for groundwater samples from Portimão–Estombar area (*sector I*). The symbols (●) stands for the Estombar springs and (○) stands for boreholes. The line (...) stands for the seawater–fresh water mixing line, and (—) represents the regression line.

coast line and the mean composition of the groundwater (water samples with electrical conductivity below 1000 μS/cm) as reference for the "initial isotopic and physico-chemical composition" ($\delta^2H = -26.04‰$; $\delta^{18}O = -4.24‰$; E. Cond. = 807 μS/cm), the percentage of seawater was calculated for different selected water sampling points using the following equation (Table 2):

$$X = [(C_{(m)} - C_{(0)})/(C_{(sea)} - C_{(0)})] \times 100 \quad (3)$$

where X stands for the percentage of seawater in the mixture, $C_{(m)}$ the composition in the mixture; $C_{(0)}$ the same parameter in the groundwater mean value, and $C_{(sea)}$ stands for the concentration in the sea. The percentage of seawater obtained for the same groundwater "point" are in agreement using the isotopic values ($\delta^{18}O$ and δ^2H), the physical (electrical conductivity) and the chemical parameters (chloride). The values similarity within the "same point" (percentage of seawater) using the different parameters is indicative of a sea–fresh water mixing mechanism as the main mechanism responsible for the groundwater mineralization.

The results obtained are in agreement with the work presented by Geirnaert et al. (1986), performed in the same research area, which had also applied stable isotopes ($\delta^{18}O$ and δ^2H) as a tool to identify the origin of salts in groundwater, with a transition zone of about 1.5 km inland. Corroborating seawater intrusion as the main mechanism responsible for groundwater mineralization increase, the relatively high tritium (5–8 TU) measured in the groundwater samples indicates that the mixing process is still active and that the fresh water component is modern. On the other hand, the Portuguese Network Isotopes in Precipitation initiated in 1988 obtained at Faro Meteorological Station (Algarve) tritium content varying between 14.8 ± 1.4 TU (June 1988) and 4.7 ± 0.7 TU (November 1989) in monthly precipitation samples. Recent data points to a tritium average content in Portuguese mainland near the coast to be 4.5 TU (Carreira et al., 2006).

(ii) *Case Study II: Faro–Tavira*

This second sector is located near the Spanish border in the eastern part of the Algarve basin (Fig. 2). Faro–Tavira zone is the main agricultural region of the Algarve. According to Stigter et al. (1998) the different groundwater *facies* found in the Faro

Table 2
Percentage of seawater in the groundwater systems from Portimão–Estombar (*Study area I*) and Faro–Tavira (*Study area II*). The data represent the amount of seawater estimated in percentage from the different tracers at the different sampling sites.

Sector	Sample reference	$\delta^{18}O \pm \upsilon$ (%)	δ^2H (%)	E. Cond. (%)	Cl^- (%)
Portimão–Estombar (*sector I*)	061	4.8 ± 2.1	4.4	5.0 ± 1.0	5.5
	062	8.6 ± 2.1	6.7	4.2 ± 1.0	3.6
	062a	5.7 ± 2.1	n.a.	8.3 ± 1.0	n.a.
	072	12.6 ± 2.1	12.2	13.5 ± 1.0	12.4
	073	8.8 ± 2.1	10.3	10.7 ± 0.8	9.5
	074	14.4 ± 2.1	14.9	18.4 ± 1.3	17.0
	075	15.1 ± 2.1	16.8	18.5 ± 1.3	17.1
	099	7.7 ± 2.1	n.a.	10.8 ± 1.0	n.a.
Faro–Tavira (*sector II*)	039	2.4 ± 2.1	3.0	11.9 ± 0.9	11.7
	043	2.8 ± 2.1	3.6	9.6 ± 0.7	8.6
	044	12.3 ± 2.1	19.6	17.0 ± 1.2	15.1
	044	10.8 ± 3.1	n.a.	14.4 ± 1.0	n.a.
	044	12.5 ± 3.1	n.a.	12.0 ± 0.9	n.a.
	044	9.9 ± 3.0	n.a.	18.6 ± 1.3	16.5
	045	7.4 ± 2.1	6.9	9.0 ± 0.7	7.7

Notes – n.a. stands for not analyzed; E. Cond. stands for electrical conductivity.

area is the result of several hydrochemical processes, sometimes having a natural origin, often affected or induced by human activities, which can involve agricultural practices. Those authors mentioned the importance of evapotranspiration of infiltrating rainwater in this region, and the role played by dissolution of calcite, dolomite and gypsum in the chemical composition of groundwater (Fig. 4).

The dispersion of the groundwater samples observed in the Piper diagram (Fig. 4) is evident in the cations content. In the cation domain of the Piper diagram, samples are spread by the vertices of the triangle. The same is not true in the anion domain, where most of the samples are distributed between the HCO_3 and Cl, that is, between the average composition of the groundwaters from Faro–Tavira sector and the average composition of seawater. This distribution indicates that seawater intrusion should be seen as the main mechanism responsible for the high observed salinity.

In this study region, even where high nitrates concentrations are a signature of agricultural activities at many sites (e.g., Carreira, 1991), most of the studied groundwater samples have values on or near the Global Meteoric Water Line (G-MWL). Only one sample (No. 38) is isolated and plotted on the sea–fresh water mixing line (Fig. 5a and b). The fresh water component of Faro–Tavira area represents the mean isotopic and chemical data obtained with the groundwater samples with lower mineralization (electrical conductivity $\leqslant$1000 μS/cm (n = 16)). Near the coastline, boreholes were identified with high Cl^- concentration and high electrical conductivity values, which could be associated either with mixing with seawater due to intensive pumping activities near the coast or with salts dissolution.

Plotting the electrical conductivity (EC) of the groundwater samples as a function of the isotopic composition ($\delta^{18}O$) different scenarios can be observed (Fig. 5b). It seems that the increase of salt concentration is not accompanied by an isotopic effect: dissolution of salt minerals appears to be the prevailing mechanism of groundwater salinization rather than seawater intrusion. Supporting this hypothesis is the discrepancy of seawater percentage obtained using either the isotopic composition or the physico-chemical data (see Table 2, samples 039 and 043). Moreover, the correlation coefficient between $\delta^{18}O$ and electrical conductivity is poor (r = 0.26; n = 48) pointing to a salt origin other than sea.

A particular case in this area is that of Fuseta spring (sample 44(ϕ) – see Table 1 (Faro–Tavira), having very low discharge rate, high and variable salinity, and slightly enriched $\delta^{18}O$ values. However, given the relationship between the groundwater mineralization and its isotopic composition (EC = 9550 μS/cm – $\delta^{18}O$ = −3.74‰; EC = 8230 μS/cm – $\delta^{18}O$ = −3.64‰; EC = 7000 μS/cm – $\delta^{18}O$ = −3.55‰ and EC = 10,400 μS/cm – $\delta^{18}O$ = −3.93‰), seawater intrusion does not appear to be the only important mechanism responsible for the groundwater salinization. I.e., both processes such as dissolution of salt minerals and mixing with seawater, should be present in this water sampling point: in this part of Algarve region evaporitic minerals such as halite are observed in the sedimentary layers as dispersed or as small concentrations of salts (Costa et al., 1985). To corroborate the hypothesis of different salt origin, different percentages of seawater were obtained from Eq. (3), using either the isotopes or the EC or Cl^- content, for the water sampling points with the highest mineralization (Table 2).

One plausible hypothesis for the ^{18}O enrichment observed in three groundwater samples (Fig. 5b) is evaporation of irrigation water, which also leads to a small increase of water salinization. Transpiration processes imply a largely prevalent, almost unidirectional, movement of water from soil to plant leaves and atmosphere, and do not affect significantly the isotopic composition of groundwater (Clark and Fritz, 1997). Soil evaporation is a complex process: in hyper-arid terrestrial environments the process consists again in a unidirectional water transfer from the water table

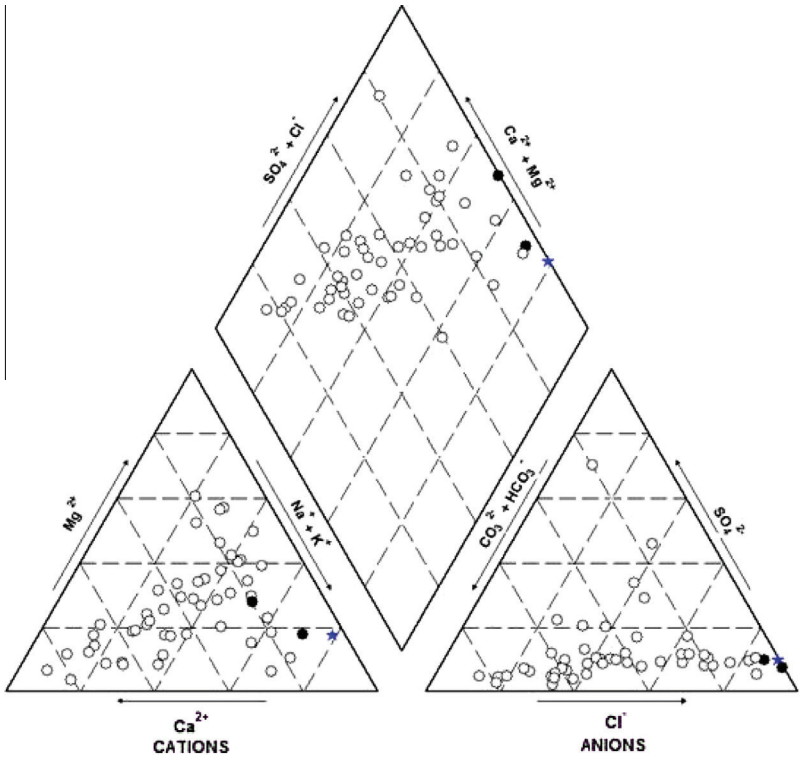

Fig. 4. Piper diagram of hydrochemical data from Faro–Tavira sector. (○) Stands for the groundwater samples; (●) stands for Fuseta spring and (★) for seawater mean composition.

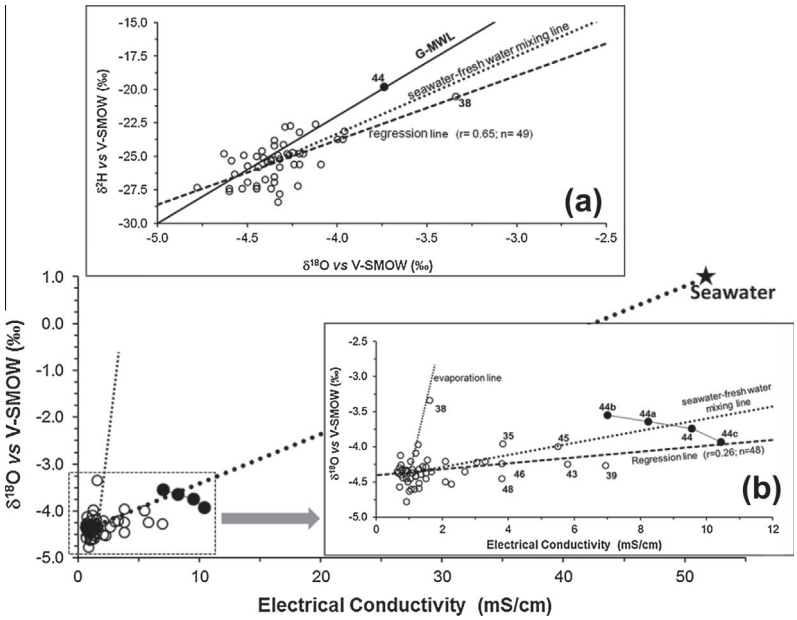

Fig. 5. (a) δ^2H *vs.* $\delta^{18}O$; (b) $\delta^{18}O$ *vs.* electrical conductivity for groundwater samples from Faro–Tavira area (*sector II*). The symbols (●) stands for the Fuseta spring and (○) stands for boreholes. The line (. . .) stands for the seawater–fresh water mixing line, and (—) represents the regression line.

to the atmosphere, not affecting the isotopic composition of groundwater (Mook, 2000). In humid areas, the infiltration of precipitation determines a mixing of rainwater with water enriched in heavy isotopes in the upper soil layers, which may in some cases affect the isotopic composition of groundwater. However, this effect is usually limited. For coastal areas, seawater ratios are maintained in the combination of dry and wet salts deposition while evaporation may cause a deviation in the isotopic composition of the groundwater, which results in enrichment of ^{18}O and ^{2}H in the remaining water (Horita, 2005).

4. Case study: Lower Tagus–Lower Sado basin, central Portugal

4.1. Hydrogeological setup

The Lower Tagus–Lower Sado basin is located in Lisbon–Setúbal region and represents an important water resource for this large region (Fig. 6a). The highly industrialized and populated urban areas of Setúbal and Lisbon are supplied by this system, which has been extensively exploited over the last decades. In order to find out the source of salinization in these groundwater systems, chemical (Cl^-, HCO_3^-, SO_4^{2-}, Ca^{2+}, Mg^{2+}, Na^+ and K^+) and isotopic (δ^2H, $\delta^{13}C$, $\delta^{18}O$, ^3H and ^{14}C) analyses were performed on groundwater samples collected in 40 boreholes (Fig. 6b). In this region there is a growing concern that these groundwater systems maybe threatened by further (uncontrolled) exploitation, due to mixing with highly polluted shallow aquifers, seawater intrusion processes in the coastal areas, or by brine dissolution detected at depth by geophysical studies (Astier, 1979).

From the geological point of view, the Lower Tagus–Lower Sado basin is characterized by a huge synclinal structure composed of Tertiary sediments, mainly formed by marine deposits (Simões, 2003). Three main groundwater systems can be identified in the region:

(i) A shallow Quaternary aquifer constituted by alluvial deposits presenting high transmissivity values.
(ii) Fluvial terraces made out of sands and clays representing the Pliocene layers.
(iii) Miocene deposits composed of sandstones and limestones of marine origin, related with different marine transgression and regression events. These deposits show an average thickness around 200–300 m, although in the central part of the basin the values increase up to 800 m (Simões, 2003).

Geophysical studies performed in the Lisbon–Setúbal region reveal two important fault systems (Astier, 1979). The first is located in the Lower Tagus valley, with a N30°E direction, and the other one, the so-called Setúbal–Pinhal Novo fault system, runs N–S and is responsible for a graben structure. This tectonic structure allowed the rise of a saline formation at depth detected by geophysical studies, which indicate the hypothesis of a brine formation unit; ancient seawater trapped in the sediments or a diapiric structure at depth (Fig. 6a). This third region is located near Lisbon and is one of the most industrialized locations of Portugal, but is surrounded by agricultural fields.

4.2. Isotopic signatures

The mean isotopic composition of the groundwater (water samples with electrical conductivity below 300 μS/cm ($n = 10$)) was used as reference for the "initial isotopic and physic-chemical composition", representing the freshwater component. Most groundwater samples are plotted above or near the G-MWL (Fig. 7a). However, seven samples (2b, 3a, 3b, 6, 42a, 42b and 43) exhibit a distinctive isotopic composition and define an approximately parallel line to the GMWL. One possible explanation for this shift is infiltration/recharge under different climatic conditions, indicating a palaeoclimatic effect within this groundwater group. The observed isotopic shift might be associated with preferential storage of isotopically depleted water in the polar ice caps. The isotopic composition of the oceans is assumed that have changed by 1.3–1.6‰ in ^{18}O and about 10‰ in deuterium during glacial times (Rozanski, 1985; Chappell and Shackleton, 1986). The significance of stable isotopes (^{18}O and ^{2}H) as climatic fingerprints and their application to palaeohydrologic and palaeoclimatic studies have been discussed by various workers worldwide (Darling et al., 1997; Edmunds and Wright, 1979). Present-day representative

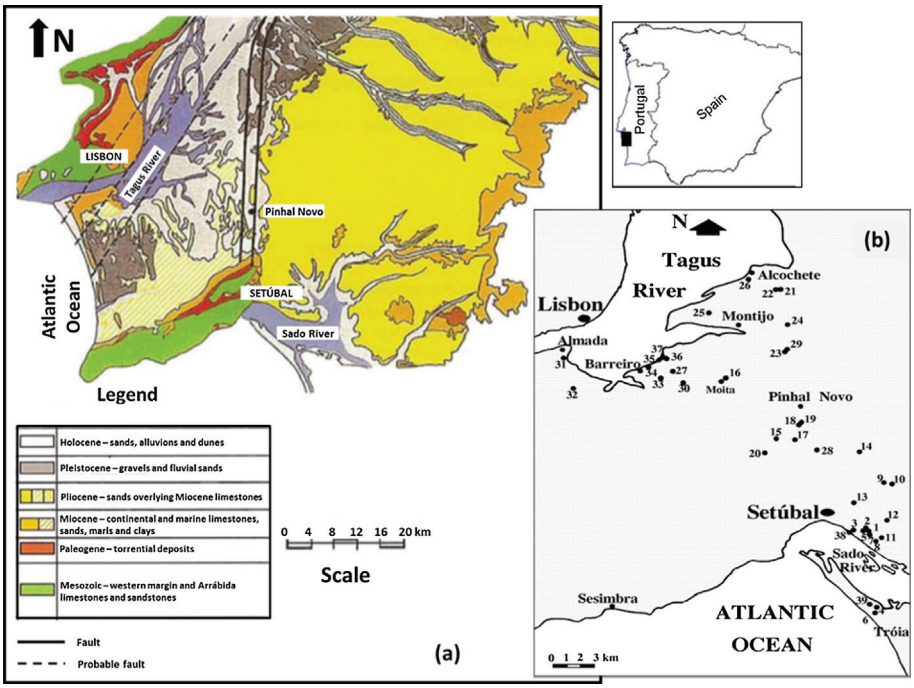

Fig. 6. (a) Lower Tagus–Lower Sado basin geology and tectonics (adapted from Simões, 2003). (b) Location of the sampling sites.

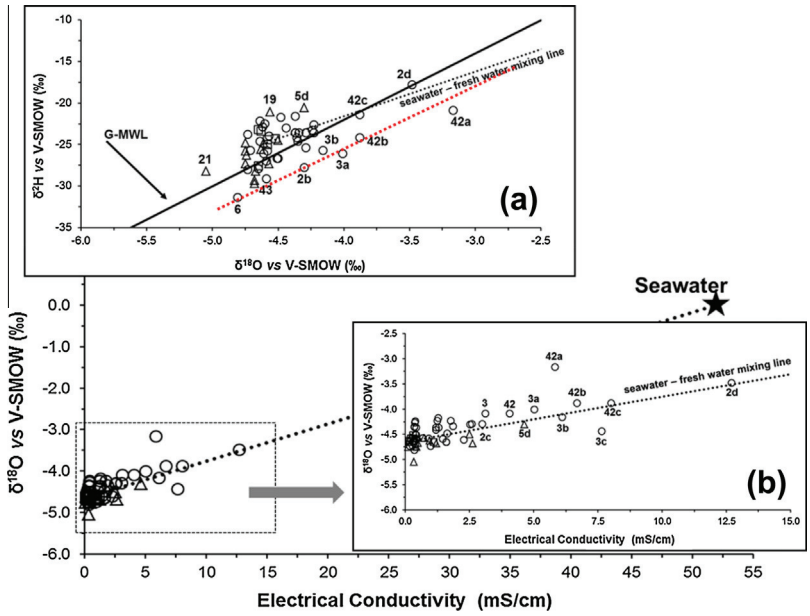

Fig. 7. (a) δ^2H *vs.* $\delta^{18}O$; (b) $\delta^{18}O$ *vs.* electrical conductivity for groundwater samples from Lower Tagus–Lower Sado basin. (○) Stands for groundwater samples from Miocene aquifer; (Δ) stands for Mio-Pliocene groundwater samples and (□) stands for Pliocene groundwater samples.

values of oxygen-18 and deuterium observed in precipitation, may be used as sensitive indicators of change and complexity in past temperature; precipitation patterns and air mass circulation. In plots of $\delta^{18}O$ as a function of the electrical conductivity (Fig. 7b), sample 2d shows the highest mineralization (see Table 3) and is located on the seawater–fresh water mixing line, followed by the samples 42c, 3c 42b and 3b. No tritium was found in most of the groundwater samples representing the Miocene aquifer system, while in the shallow Pliocene aquifer the tritium content varies between 1 and 3 TU (Table 3). Radiocarbon determinations were carried out on the Total Dissolved Inorganic Carbon (TDIC). The ^{14}C content varies from 71.9 ± 0.7 to 88 ± 0.8 pmC in the Pliocene groundwater samples, and from 2.9 ± 0.3 up to 45.6 ± 0.9 pmC in the Miocene groundwater samples.

To estimate the apparent ^{14}C age (Eqs. (1) and (2)), the value of $\delta_S = -23 \pm 2‰$ was adopted for calculating the initial ^{14}C activity Eq. (2). It should be noted that the soil CO_2 is enriched in ^{13}C with respect to the organic matter being decomposed, as well as with respect to CO_2 respired by roots of living plants, by 4‰ due to kinetic fractionation associated with diffusion of this gas from the soil to the atmosphere (Dörr and Münnich, 1980, 1987). The value of 0 ± 1‰ was adopted as representative for the soil and rock

Table 3
Lower Tagus–Lower Sado basin, central Portugal: isotopic data and some physico-chemical parameters ascribed to the groundwater sampling sites.

Sample ref.		EC (μS/cm)	Cl (mg/L)	$SI_{(calc.)}$	$SI_{(dol.)}$	$SI_{(gyps.)}$	$\delta^{18}O$ (‰)	$\delta^{2}H$ (‰)	^{3}H (TU)	$\delta^{13}C$ (‰)	^{14}C (pmC ± σ)	Apparent age BP (ka)
1	(M)	2592	719	0.373	0.274	−1.561	−4.29	−23.6	0			
2	(M)	1277	312	0.101	−0.345	−1.880	−4.18					
2a	(M)	1776					−4.23	−22.6	1.45			
2b	(M)	2530	710	0.161	−0.042	−1.515	−4.30	−27.8	0			
2c	(M)	3000	809	0.068	−0.348	−1.241	−4.29	−25.4	0	−10.4	12.9 ± 0.9	14.6 ± 2.8
2d	(M)	12,707	4054	0.464	0.930	−0.657	−3.48	−17.8	0			
3	(M)	3111	916	0.160	−0.137	−1.410	−4.09	–				
3a	(M)	5030					−4.01	−26.1	0	−9.2	8.4 ± 0.8	17.2 ± 3.0
3b	(M)	6105	2095	0.558	0.803	−0.786	−4.16	−25.7	0			
3c	(M)	7650	2485	0.053	−0.093	−1.168	−4.44	−23.0	1.4	−7.3	6.7 ± 0.6	17.1 ± 3.1
3d	(M)	1636	42	0.275	0.493	−1.413	−4.48	−21.7	0	−10.0	2.9 ± 0.3	26.6 ± 3.1
4	(M)	986	219	0.100	0.420	−2.230	−4.73	−28.0	1.3	−12.1	5.9 ± 0.5	22.3 ± 2.9
5	(P)	411	103	−2.459	−4.948	−2.947	−4.58					
5a	(P)	951					−4.63	−25.6	0.3			
5b	(P)	1210	334	−1.834	−3.536	−2.003	−4.68	−29.7	0			
5c	(P)	2630	738	−2.199	−4.310	−1.592	−4.68	−29.3	0	−17.9	88.1 ± 0.8	3.2 ± 2.5
5d	(P)	4631	1375	−2.628	−4.896	−1.417	−4.30	−20.6	1.4			
6	(M)	349	41	0.214	0.520	−2.655	−4.81	−31.4				
7	(M)	1243	300	0.266	0.177	−2.031	−4.23	−23.6				
8	(M)	380	43	0.109	−0.316	−2.896	−4.27					
8a	(M)	383					−4.24	−23.3	0			
8b	(M)	431	46	0.355	0.429	−2.793	−4.51	−26.7	0.8			
8c	(M)	419	55	0.214	−0.056	−2.641	−4.37	−21.6				
9	(M-P)	295	25	−0.483	−1.387	−2.818	−4.52	−24.3	1			
10	(M-P)	179	26	−2.795	−5.612	−3.537	−4.73	−23.8				
11	(M)	348	28	0.075	0.032	−2.822	−4.36	−24.2				
12	(M-P)	164	30	−3.787	−7.397	−4.012	−4.65	−23.2	1.2			
13	(M-P)	216	35	−2.333	−5.063	−3.235	−4.58	−24.4				
14	(M-P)	151	25	−2.805	−5.698	−3.861	−4.63	−23.4				
15	(P)	109	40	−4.011	−8.094	−4.012	−4.75	−25.8				
16	(M-P)	323	46	−1.307	−3.061	−2.965	−4.58	−25.0				
17	(P)	383	32	−0.086	−1.030	−2.835	−4.71	−25.7	1.4			
18	(P)	168	31	−3.394	−6.806	−3.722	−4.61	−24.8	1.6			
19	(P)	209	40	−3.859	−7.629	−3.719	−4.56	−21.1				
21	(P)	342	46	−1.368	−3.293	−2.718	−5.05	−28.2	2.6	−17.6	71.9 ± 0.7	4.8 ± 2.5
22	(P)	448	84	−2.125	−4.174	−2.942	−4.75	−24.8				
23	(P)	746	112	−1.690	−3.227	−2.294	−4.57	−27.3				
24	(P)	494	88	−1.946	−3.820	−2.810	−4.67	−28.2				
25	(M)	396	33	0.104	−0.434	−2.697	−4.50	−26.7				
26	(P)	425	82	−3.807	−7.584	−2.892	−4.74	−26.3				
27	(P)	2507	1400	−2.214	−4.232	−1.850	−4.50	−24.5	0	−10.0	85.6 ± 3.3	Modern
28	(M)	447	39	−0.620	−1.797	−2.538	−4.59	−27.0				
29	(P)	441	95	−2.543	−4.970	−3.128	−4.75	−27.3				
30	(M)	281	28	−0.681	−1.942	−2.975	−4.64	−24.6				
31	(M)	1860	294	0.151	−0.163	−1.430	−4.34	−23.6	0	−10.5	45.8 ± 0.6	4.2 ± 2.6
32	(M-P)	1112	144	−0.446	−1.534	−2.288	−4.65	−27.6	0	−12.9	32.8 ± 0.5	8.7 ± 2.5
33	(M)	437	61	−0.129	−0.626	−2.646	−4.60	−22.5				
34	(M)	693	110	−2.520	−5.616	−2.264	−4.57	−24.0				
35	(M)	352	33	−0.128	−0.816	−2.943	−4.64	−22.2				
36	(M)	362	26	−0.094	−0.748	−2.773	−4.62	−22.9				
37	(M)	361	27	−0.014	−0.586	−2.893	−4.35	−24.6				
38	(M)	2281	469	0.142	0.298	−1.201	−4.61	−26.1				
39	(M)	919	203	0.054	0.177	−2.201	−4.58	−25.8	0	−10.0	10.8 ± 0.7	15.8 ± 2.8
42	(M)	4056	1193	0.177	0.195	−1.293	−4.09					
42a	(M)	5820					−3.17	−20.9	0	−8.1	5.6 ± 1.2	19.5 ± 4.4
42b	(M)	6677	2050	0.573	1.084	−0.895	−3.88	−24.2	0			
42c	(M)	8010	2698	0.026	0.101	−1.391	−3.88	−21.4	0	–	7.1 ± 1.2	17.4 ± 3.9
43	(M)	1200					−4.41					
43a	(M)	1296					−4.37	−23.6	0	−6.95	3.1 ± 0.4	23.1 ± 3.5
43b	(M)	1450	284	0.648	1.273	−1.407	−4.59	−29.1	1.0			
43c	(M)	1592	326	−0.235	−0.582	−1.436	−4.65	−27.9	0	−7.08	4.0 ± 0.4	21.1 ± 3.2

Note: (M) – stands for Miocene; (M-P) – stands for Mio-Pliocene and (P) – stands for Pliocene. $SI_{(calc.)}$ stands for the saturation index with respect to calcite; $SI_{(dol.)}$ stands for the saturation index with respect to dolomite and $IS_{(gyps.)}$ stands for the saturation index with respect to gypsum.

carbonates for δ_R. To account for fractionation during dissolution of soil CO_2 in the infiltrating water we adopted $\varepsilon_{13} = 9.0 \pm 0.1‰$ (Mook et al., 1974).

This simple model was found appropriate, since in all analyzed water samples the saturation index (SI) with respect to calcite is not significant, and the $\delta^{13}C$ measured in the TDIC of the groundwater samples is around −10‰, pointing to a small contribution from carbonate dissolution. The estimated apparent carbon-14 ages vary between modern in the Pliocene aquifer (samples 5 and 27), and up to 26.6 ± 3.1 ka BP in the Miocene aquifer (sample 3d). The apparent groundwater ages obtained for the deepest aquifer were higher than 14.6 ± 2.8 ka BP (with exception of borehole 31), with an average age around 19 ka BP (Table 3), and so indicate the presence of palaeowaters.

The observed relationship between the apparent carbon-14 groundwater age, ^{14}C concentration and the electrical conductivity

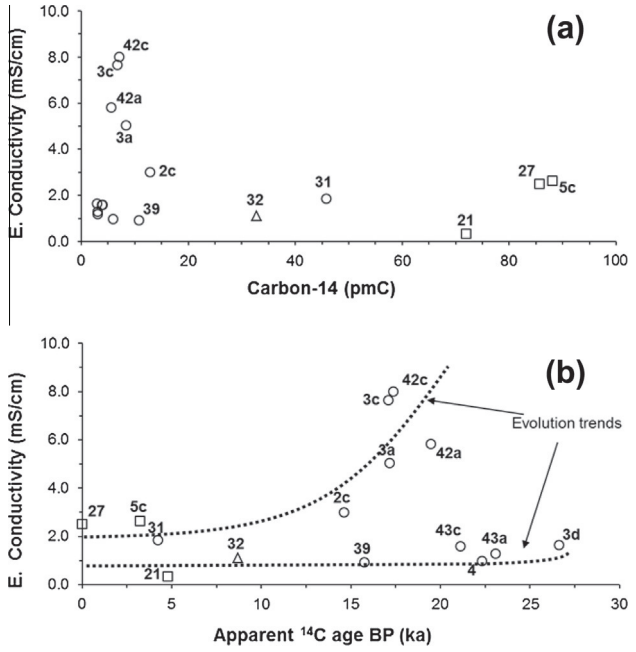

Fig. 8. Results from Lower Tagus–Lower Sado basin: (a) Electrical conductivity *vs.* carbon-14 content; (b) electrical conductivity *vs.* apparent carbon-14 groundwater age (symbols as in Fig. 7).

(or with Cl^- content) reveals two evolution trend lines (see Fig. 8a and b), recognized by the graphic pattern defined by the distribution of the samples in the diagram with the increase of salinization. These two trends may be produced by different mineralization origins: brine dissolution/evaporitic dome dissolution/ancient seawater trapped in the sediments/modern seawater intrusion, or could be ascribed to distance from the coast. In the northern part of the basin, a Pliocene phreatic aquifer near the Tagus river, modern seawater intrusion appears to play the dominant role in the water mineralization of the shallow aquifer. The salinity increase is accompanied by high percentage of modern carbon (samples 5, 21 and 27 "modern apparent groundwater ages"), i.e., in the northern part of the basin the increase of salinization is not followed by a groundwater ageing increase.

Using the application of radiocarbon measurements, stable isotopes and hydrochemical data, different approaches to explain the salts origin are possible: mixing between fresh groundwater and modern seawater leads to an increased activity. In the Sado–Tagus basin this trend is not observed for the dated samples: samples 2, 3 and 42 reveal salinization followed by ageing. In this case the increase of salts in the groundwater system may be ascribed to ancient seawater trapped in the sediments during the sedimentary basin formation (Fig. 8b). A similar effect is presented by Sukhija et al. (1996), in a research study carried out in a coastal area of Madras, India. Those authors were distinguished palaeomarine and modern seawater intrusion on the basis of a combined approach using radiocarbon and hydrogeochemical data.

4.3. Hydrogeochemistry

Hydrogeochemical evolution is characterized by a progressive increase in the TDS: from 80 mg/L up to 2565 mg/L in the Pliocene aquifer, while in the Miocene the mineralization range between 200 mg/L and 7800 mg/L. Hydrochemical evolution of groundwaters in the Sado basin is characterized by a gradual change from Ca–HCO_3 and Ca–Mg–HCO_3-type waters to a Na–Cl-type waters near the coast line. The evolution of the groundwaters towards Na–Cl-type water indicates that ion exchange and calcite/dolomite dissolution are the dominant geochemical processes in the aquifer. From the Piper diagram the projections of the groundwater samples from Sado area are distributed towards the seawater composition (Fig 9).

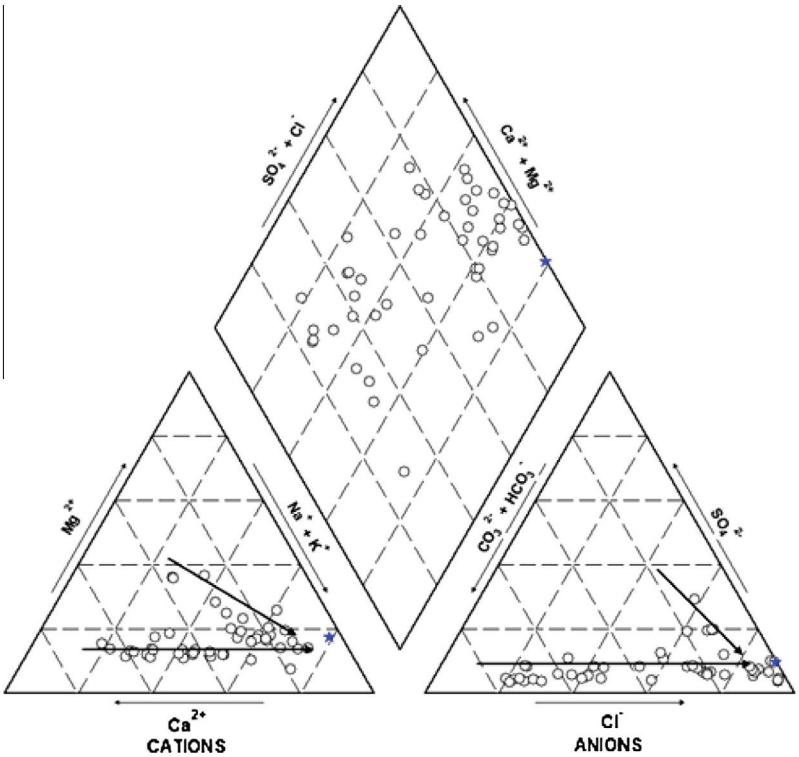

Fig. 9. Piper diagram of hydrochemical data from (○) stands for the groundwater samples and (★) for seawater mean composition.

Two different evolution trends were recognized in the ratio Ca^{2+}/Na^{+} (Fig. 10a), both apart from the seawater–fresh water mixing line, reflecting probably flow paths with different amounts of carbonate minerals. The observed trend may be also due to different ionic exchange proportions, since the ion exchange mechanism is able to influence the ion concentration of the groundwater. Also, adsorption of Na^{+} by the aquifer matrix, with release of Ca^{2+}, is a process which is triggered by intruded seawater. Applying the equation presented by Pennisi et al. (2006), the magnitude of ion exchange processes for Ca^{2+} and Na^{+}, was calculated by comparing the difference (Δn) between the measured concentration ($n_{(m)}$) and that expected by mixing with seawater ($n_{(c)}$), based on the contribution from the conservative ion Cl^{-}. The mixing equation (Eq. (4)) for ion X is:

$$\Delta n_X = n_{X(m)} - n_{X(c)}$$
$$\Delta n_X = n_{X(m)} - [n_{X(0)} + (n_{Cl(m)} - n_{Cl(0)})(n_{X(sea)}/n_{Cl(sea)})] \quad (4)$$

where $n_{X(0)}$ and $n_{Cl(0)}$ are the concentrations of ions X and Cl^{-} in groundwater not affected by sea water intrusion. In our case study, these values are the mean values obtained in the groundwater samples with an electrical conductivity below 300 μS/cm.

Since the research region is a sedimentary basin, cation exchange process can easily occur with the uptake of sodium dissolved in the groundwater with release of calcium by the aquifer matrix. Most groundwater samples present a Na^{+} deficit ($\Delta n_{Na} < 0$) and an excess of Ca^{2+} ($\Delta n_{Ca} > 0$), corroborating the hypothesis that the missing of Na^{+} and increase of Ca^{2+} is ascribed to cation exchange mechanisms (Fig. 10b). According to Appelo and Postma (1994), in coastline aquifers ions in freshwater are often derived from sea spray and only calcium and bicarbonate are added to the water due to calcite dissolution. Within the Sado basin, the Ca/Na ratio may vary greatly due to the occurrence of a heterogeneous interface, influenced by the layering of coastal aquifer system and the fact that an inland moving interface will present different geochemical effects. Mixing with ancient seawater trapped in the sediments, during the sedimentary basin formation, is probably another process affecting groundwater salinization in the south area in the research region. Here the deep groundwater system, with apparent carbon-14 ages between 15 and 20 ka and electrical conductivity reaching 10,000 μS/cm, is being "used" for public supply where it is mixed with groundwater from a system with lower mineralization.

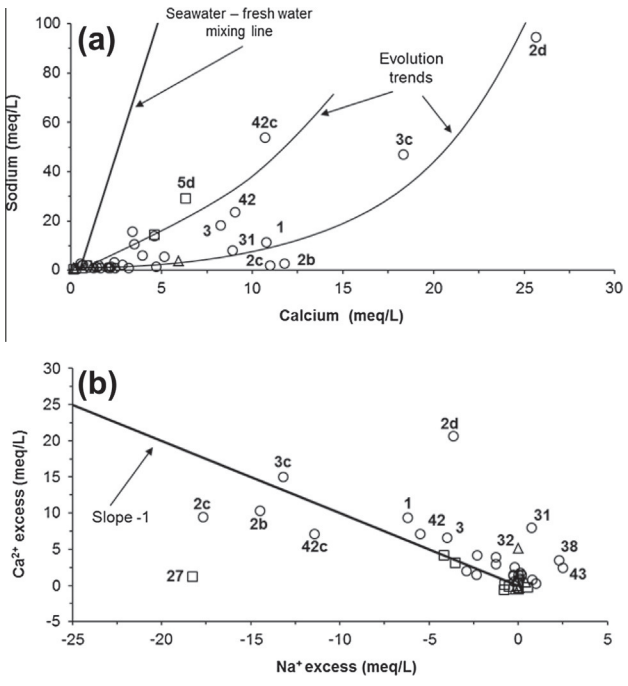

Fig. 10. Results from Lower Tagus–Lower Sado basin: (a) sodium *vs.* calcium; (b) calcium excess *vs.* Na excess in Sado–Tagus groundwaters. The replacement of Na^{+} by Ca^{+} through ion exchange is triggered by seawater (symbols as in Fig. 7).

Calcite saturation is not present in all groundwater samples collected within the Sado Basin system, most probably due to continuous increases in alkalinity as a result of exchange reactions with the ions present in clay minerals. In fact, the samples where modern seawater intrusion is present in the aquifer are those which are further from the equilibrium with calcite. Changes in groundwater chemistry inside the basin indicate that the most feasible explanation for the variation in the cation composition is related with cation exchange processes. An alternative hypothesis is that carbonate equilibrium controls the alkaline earth elements, particularly the increase in Ca^{2+} and Mg^{2+}, and or proportional sodium increase associated with the high solubility of Na^{+} salts. However, these hypotheses seems not to be reliable, in this case, because the sodium deficit associated with the calcium excess cannot be explained on the basis of the solubility of the salts of these ions. A similar "trend" was referred to in a case study in a coastal aquifer in Argentina by Martinéz and Bocanegra (2002).

5. Conclusions

The wide range of groundwater salinity problems in terms of its origin and prevention, makes necessary the use of integrated geochemical and isotopic methods to interpret salinity issues; especially in the context of the deterioration of water quality resulting from pollution or exploitation of groundwater resources. Human factors intensify salinity directly by pollution or indirectly by agricultural activities, and excessive pumping leading to invasion of saline groundwater into freshwater aquifers. Stable isotopes provide an effective label for sea water and freshwater, to enable tracing of sea water intrusion and identification of processes that may be responsible for water salinization, through the evolution of stable isotope concentrations in water during different processes related to salinization.

In the Portimão–Estombar zone, the isotopic ($\delta^{18}O$ and $\delta^{2}H$), physical (electrical conductivity), and chemical parameters (e.g. Cl^{-}), clearly evince a seawater–fresh water mixing trend. In the Faro–Tavira zone the increase of salt concentration is generally not accompanied by an isotopic effect. Here, dissolution from salt diapirs appears as the prevailing mechanism of groundwater salinization, rather than seawater intrusion. Anthropogenic causes such as overexploitation, or salinization by evaporation of irrigation water, appear to be important secondary processes, although evaporative effects are localized.

In the Lower Tagus–Lower Sado basin, two different evolution trends were recognized. Both differ from the seawater–fresh water mixing line, probably reflecting flow paths with different amounts of carbonate minerals and different ionic exchange proportions (Ca^{2+}/Na^{+}). The ion exchange mechanism is able to influence the ion concentration of the groundwater, representing the most realistic explanation for the cation variation. These variations observed in the ionic ratios can be ascribed to the occurrence of a heterogeneous interface, influenced by the layering of coastal aquifer system, and to the inland moving interface responsible for the different geochemical water types. The alternative hypothesis of carbonate equilibrium control of the alkaline earth elements, and proportional sodium increase associated with dissolution of evaporitic minerals, seems not be applicable in this case. The apparent groundwater ages estimated for the Miocene aquifer average around 19 ka BP, indicating the presence of palaeowaters. In the

northern part of the basin, modern seawater intrusion appears to play the major role in the groundwater mineralization in the shallow aquifer, since the increase of salinization is not accompanied by a groundwater ageing increase. However, in the southern area of the basin, near Setúbal, intensification of groundwater salinization was accompanied by an increase of the apparent ages. In this case the increase of salts in the groundwater system should be ascribed to ancient seawater trapped in the sediments, during the sedimentary basin formation.

The use of geochemical or isotopic data as individual tracers to identify and characterize salts origin in groundwater systems is much more effective when used in combination. In our different case studies, the joint use of joint geochemical and isotopic tracers (stable and radioactive environmental isotopes) has proved to be highly effective. The variability in chemical and isotopic composition of deep and shallow groundwater indicates that differences exist in the salts origin in groundwater systems. Further, dating groundwater helped in the identification of modern or ancient salt water bodies mixing with the freshwater system, such as seawater, brackish or brine waters. This joint geochemical and isotopic approach provided a better understanding of the variable nature of groundwater mineralization, which can help to optimize groundwater resources in the study regions.

Acknowledgments

These studies were funded by International Atomic Energy Agency – Isotope Hydrology Section under the Project POR/8/004. An early draft of this manuscript was critically read by Roberto Gonfiantini and two anonymous reviewers, and the authors would like to thank their comments and suggestions which were extremely helpful in order to improve the manuscript. The authors also would like to acknowledge Elisa Sacchi for her comments and suggestions and other anonymous reviewer for the support to develop the manuscript. The authors would like to acknowledge Christoph Burbidge for his help in English improvement.

References

Appelo, C.A.J., Postma, D., 1994. Geochemistry, Groundwater and Pollution. A.A. Balkema, Rotterdam, p. 536.

Aráguás-Aráguas, L., Gonfiantini, R., 1989. Environmental Isotopes in Sea Water Intrusion Studies. IAEA Internal Report, Vienna.

Astier, J.L., 1979. Etude des resources em eaux souterraines de la péninsule de Setúbal – Portugal. Geophysique. Nouveaux résultats de la prospection électrique. UNDP – Unesco, dir. Geral Serv. Hidraulicos. 9p.

Bouchaou, L., Michelot, J.L., Vengosh, A., Hsissou, Y., Qurtobi, M., Gaye, C.B., Bullen, T.D., Zuppi, G.M., 2008. Application of multiple isotopic and geochemical tracers for investigation of recharge, salinization, and residence time of water in the Souss–Massa aquifer, southwest of Morocco. J. Hydrol. 352, 267–287.

Cabral, J.M.P., Carreira, P.M., Vieira, M.C.R., Braga dos Santos, J., Leitão de Freitas, M.J., Gonfiantini, R., 1992. Study of groundwater salinization in Algarve, Portugal, using environmental isotope techniques. In: IAEA, Proceeding Series, Isotope Techniques in Water Resources Development, 1991, pp. 694–697.

Carol, E., Kruse, E., Mas-Pla, J., 2009. Hydrochemical and isotopical evidence of ground water salinization processes on the coastal plain of Samborombón Bay, Argentina. J. Hydrol. 365, 335–345.

Carreira, P.M., 1991. Mechanisms of Salinization of Coastal Aquifers in the Algarve. MSc Thesis, ICEN/INETI, p. 143 (in Portuguese).

Carreira, P.M., Macedo, M.E., Soares, A.M.M., Vieira, M.C., Santos, J.B., 1994. Origin of salinization of the aquifer system of the Lower Sado Basin, in the region of Setubal. Recursos Hídricos 15 (1), 41–48 (in Portuguese).

Carreira, P.M., Marques, J.M., Graça, R.C., Aires-Barros, L., 2008. Radiocarbon application in dating "complex" hot and cold CO_2-rich mineral water systems: a review of case studies ascribed to the northern Portugal. Appl. Geochem. 23, 2817–2828.

Carreira, P.M., Marques, J.M., Pina, A., Mota Gomes, A., Galego Fernandes, P.A., Monteiro Santos, F., 2010. Groundwater assessment at Santiago Island (Cabo Verde): a multidisciplinary approach to a recurring source of water supply. Water Resour. Manage. 24, 1139–1159.

Carreira, P.M., Valério, P., Nunes, D., Araújo, M.F., 2006. Temporal and seasonal variations of stable isotopes (δ^2H and $\delta^{18}O$) and tritium in precipitation over Portugal. In: Proceedings of IAEA. Conference Isotopes in Environmental Studies, pp. 370–373.

Cartwright, I., Weaver, T.R., Fulton, S., Nichol, C., Reid, M., Cheng, X., 2004. Hydrogeochemical and isotopic constraints on the origins of dryland salinity, Murray Basin, Victoria, Australia. Appl. Geochem. 19, 1233–1254.

Cartwright, I., Weaver, T.R., Keith Fifield, L., 2006. Cl/Br ratios and environmental isotopes as indicators of recharge variability and groundwater flow: an example from the southeast Murray Basin, Australia. Chem. Geol. 231, 38–56.

Carvalho, M.R., Almeida, C., 1989. HIDSPEC, um programa de especiação e cálculo de equilíbrios água/rocha. Rev. Univ. Aveiro 4 (2), 1–22.

Chappell, J., Shackleton, N.J., 1986. Oxygen isotopes and sea level. Nature 324, 137–140.

Clark, I.D., Fritz, P., 1997. Environmental Isotopes in Hydrogeology. Lewis Publishers, New York.

Costa, F.E., Brites, J.A., Pedrosa, M.Y., Silva, A.V., 1985. Hydrogeological Map of Algarve Basin. Descriptive News 1:100000. Serviços Geológicos de Portugal. 95 p. (in Portuguese).

Craig, H., 1961. Isotopic variations in meteoric waters. Science 133 (3465), 1702–1703.

Custódio, E., Llamas, M.R., 1983. Hidrologia subterránea. Tomo 1, second ed., Barcelona, 1157p.

Dansgaard, W., 1964. Stable isotopes in precipitation. Tellus XVI 4, 436–468.

Darling, W.G., Edmunds, W.M., Smedley, P.L., 1997. Isotopic evidence of palaeowaters in the British Isles. Appl. Geochem. 12, 813–829.

Dörr, H., Münnich, K.O., 1980. Carbon-14 and carbon-13 in soil CO_2. Radiocarbon 22, 909–918.

Dörr, H., Münnich, K.O., 1987. Annual variations in soil respiration in selected areas of the temperate zone. Tellus 39B, 114–121.

Edmunds, W.M., 2005. Groundwater as an archive of climatic and environmental change. In: Aggarwal, P.K., Gat, J.R., Froehlich, K.F.O. (Eds.), Isotopes in the Water Cycle. Past Present and Future of a Developing Science. Springer, The Netherlands, pp. 341–352.

Edmunds, W.M., Droubi, A., 1998. Groundwater Salinity and Environmental Change. Isotope Techniques in the Study of Past and Current Environmental Changes in the Hydrosphere and Atmosphere. IAEA, Vienna, pp. 503–518.

Edmunds, W.M., Wright, E.P., 1979. Groundwater recharge and palaeoclimate in the Sirte and Kufra basins, Libya. J. Hydrol. 40, 215–241.

Epstein, S., Mayeda, T., 1953. Variation of ^{18}O content of waters from natural sources. Geochim. Cosmochim. Acta 4, 213–224.

Friedman, I., 1953. Deuterium content of natural waters and other substances. Geochim. Cosmochim. Acta 4, 89–103.

Fritz, P., 1981. River waters. In: IAEA (Ed.), Stable Isotope Hydrology: Deuterium and Oxygen-18 in the Water Cycle. IAEA, Vienna, pp. 177–201.

Gat, J., 1981. Properties of the isotopic species of water: the "isotopic effect". In: IAEA, (Ed.), Stable Isotope Hydrology: Deuterium and Oxygen-18 in the Water Cycle, IAEA; Vienna, 7-19.

Gaye, C.B., 2001. Isotope techniques for monitoring groundwater salinization. In: Proceedings First International Conference on Saltwater Intrusion and Coastal Aquifers – Monitoring, Modeling, and Management. Essaouira, Morocco. 10p.

Geirnaert, W., Radstake, F., Kleinendorst, T., 1986. A salinization mechanism for springs at Estombar, Algarve, Portugal. Comun. Serv. Geol. Portugal T. 72 (1/2), 59–69.

Gonfiantini, R., Araguás, L.A., 1988. Los isotopos ambientales en los estudios de la intrusion marina. Proc. Symp. Tecnológia de la Intrusión en acuíferos Costeros, Ponencias Internacionales, 1, IGME, Madrid, 135-190.

Gonfiantini, R., Zuppi, G.M., 2003. Carbon isotopic exchange rate of DIC in karst groundwater. Chem. Geol. 197, 319–336.

Gourcy, L.L., Groening, M., Aggarwal, P.K., 2005. Stable oxygen and hydrogen isotopes in precipitation. In: Aggarwal, P.K., Gat, J.R., Froehlich, K.F.O. (Eds.), Isotopes in the Water Cycle. Past Present and Future of a Developing Science. Springer, The Netherlands, pp. 39–51.

Horita, J., 2005. Saline waters. In: Aggarwal, P.K., Gat, J.R., Froehlich, K.F.O. (Eds.), Isotopes in the Water Cycle, Past, Present and Future of a Developing Science. Springer, The Netherlands, pp. 271–287.

IAEA, 1976. Procedure and Technique Critique for Tritium Enrichment by Electrolysis at IAEA Laboratory. Technical Procedure n°19. International Atomic Energy Agency, Vienna.

Jalali, M., 2007. Salinization of groundwater in arid and semi-arid zones: an example from Tajarak, western Iran. Environ. Geol. 52, 1133–1149.

Kim, Y., Lee, K.-S., Koh, D.-C., Lee, D.-H., Lee, S.-G., Park, W.-B., Koh, G.-W., Woo, N.-C., 2003. Hydrogeochemical and isotopic evidence of groundwater salinization in a coastal aquifer: a case study in Jeju volcanic island, Korea. J. Hydrol. 270, 282–294.

Klein-BenDavid, O., Gvirtzman, H., Katz, A., 2005. Geochemical identification of fresh water sources in brackish groundwater mixtures; the example of Lake Kinneret (Sea of Galilee), Israel. Chem. Geol. 214, 45–59.

Koh, D.-C., Ha, K., Lee, K.-S., Yoon, Y.-Y., Ko, K.-S., 2012. Flow paths and mixing properties of groundwater using hydrogeochemistry and environmental tracers in the southwestern area of Jeju volcanic island. J. Hydrol. 432–433, 61–74.

Lopes, F., 2006. Rocha da Pena (Loulé, Algarve): Ao encontro da Geodiversidade. <http://rochadapena.no.sapo.pt> (11.14.12).

Lucas, L.L., Unterweger, M.P., 2000. Comprehensive review and critical evaluation of the half-life of tritium. J. Res. Natl. Inst. Technol. 105, 541–549.

Martinéz, D.E., Bocanegra, E.M., 2002. Hydrogeochemistry and cation-exchange processes in the coastal aquifer of Mar Del Plata, Argentina. Hydrogeol. J. 10, 393–408.

Mas-Pla, J., Font, E., Astui, O., Menció, A., Pérez-Paricio, A., 2013. Tracing stream leakage towards an alluvial aquifer in a mountain basin using environmental isotopes. Appl. Geochem. 32, 85–94.
Möller, P., Rosenthal, E., Geyer, S., Guttman, J., Dulski, P., Rybakov, M., Zilberbrand, M., Jahnke, C., Flexer, A., 2007. Hydrochemical processes in the lower Jordan valley and in the Dead Sea area. Chem. Geol. 239, 27–49.
Mook, W.G., 2000. Environmental Isotopes in Hydrological Cycle. Principles and Applications. IHP-V, Technical Documents in Hydrology (UNESCO/IAEA), vol. I, p. 39.
Mook, W.G., Bommerson, J.C., Staverman, W.H., 1974. Carbon isotope fractionation between dissolved bicarbonate and gaseous carbon dioxide. Earth Planet. Sci. Lett. 22, 169–176.
Pennisi, M., Bianchini, G., Muti, A., Kloppmann, W., Gonfiantini, R., 2006. Behaviour of boron and strontium isotopes in groundwater–aquifer interactions in Cornia Plain (Tuscany, Italy). Appl. Geochem. 21, 1169–1183.
Pulido-Leboeuf, P., 2004. Seawater intrusion and associated processes in a small coastal complex aquifer (Castell de Ferro, Spain). Appl. Geochem. 19, 1517–1527.
Rozanski, K., 1985. Deuterium and oxygen-18 in European groundwaters – links to atmospheric circulation in the past. Chem. Geol. (Isotope Geosci. Sect.) 52, 349–363.
Rozanski, K., Araguás-Araguás, L., Gonfiantini, R., 1992. Relation between long-term of oxygen-18 isotope composition of precipitation and climate. Science 258, 981–985.
Salem, O., Visser, J.M., Deay, M., Gonfiantini, R., 1980. Groundwater flow patterns in western Lybian Arab Jamahitiya evaluated from isotope data. In: International Atomic Energy Agency (Eds.), Arid Zone Hydrology: Investigations with Isotope Techniques, pp. 165–179.
Shi, J.A., Wang, Q., Chen, G.J., Wang, G.Y., Zhang, Z.N., 2001. Isotopic geochemistry of the groundwater system in arid and semiarid areas and its significance: a case study in Shiyang River basin, Gansu province, northwest China. Environ. Geol. 40 (4–5), 557–565.
Silva, A.V., Portugal, A., Freitas, L., 1986. Groundwater flow model and salinization of coastal aquifers between Faro and Fuseta. Comun. Ser. Geol. Portugal 72 (1/2), 71–87 (in Portuguese).
Simões, M., 2003. On the hydrogeology of the Lower Tagus Basin and its Cenozoic geologic evolution. Ciências Terra, Rev. Univ. Nova de Lisboa 15, 239–248.
Stigter, T.Y., van Ooijen, S.P.J., Post, V.E.A., Appelo, C.A.J., Carvalho Dill, A.M.M., 1998. A hydrogeological and hydrochemical explanation of the groundwater composition under irrigated land in a Mediterranean environment, Algarve, Portugal. J. Hydrol. 208, 262–279.
Stute, M., Forser, M., Frischkorn, H., Serejo, A., Clark, J.F., Schlosser, P., Broecker, W.S., Bonani, G., 1995. Cooling of tropical Brazil (5 °C) during the last glacial maximum. Science 269, 379–383.
Sukhija, B.S., Varma, V.N., Nagabhushanam, P., Reddy, D.V., 1996. Differentiation of palaeomarine and modern seawater intruded salinities in coastal groundwaters (of Karaikal and Tanjavur, India) based on inorganic chemistry, organic biomarker fingerprints and radiocarbon dating. J. Hydrol. 174, 173–201.
Yurtsever, Y., 1997. Role and contribution of environmental tracers for study of sources and processes of groundwater salinization. Hydrochem. Proc. Rabat Symp., IAHS Publ. 244, 3–12.